研究論文

Study of Runaway Electron Transport in Edge Stochastic Magnetic Field in the JFT-2M Tokamak

KAWASHIMA Hisato, NAGASHIMA Keisuke, TAMAI Hiroshi, MIURA Yukitoshi, SHOJI Teruaki, FUJITA Takaaki and MORI Masahiro
SAKURAI Shinji*, UESUGI Yoshihiko* and TAKAMURA Shuichi*

Department of Fusion Plasma Research, Japan Atomic Energy Research Institute, Ibaraki, 311-01.
**Department of Electrical Engineering, Faculty of Engineering, Nagoya University, Nagoya, 464-01.*

(Received 13 January 1994/revised manuscript: received 23 June 1994)

Abstract

The radial transport of runaway electrons has been studied in ohmically heated JFT-2M plasmas with an externally applied helical magnetic field. Clear decreases in both the hard x-ray emission and edge electron temperature are observed with application of the external helical magnetic field. This indicates that the transport of both runaway electrons and electron thermal energy is enhanced at the edge stochastic magnetic field produced by the external helical field. The diffusion coefficient of runaway electrons is evaluated in the core and the edge from the temporal behavior of the hard x-ray emission. The diffusion coefficient in the edge stochastic magnetic field is about $D_s = 1\mathrm{m}^2/\mathrm{s}$ with a radial field strength of $|B_r|/B_t \sim 2 \times 10^{-3}$. This is four orders of magnitude smaller than that predicted by the transport along the stochastic magnetic field. The large shift of the drift surface of such high energy electrons from the magnetic surface may explain this significant reduction in transport. On the other hand, the enhancement of the thermal diffusivity in the presence of the helical field is consistent with the theoretical prediction.

Keywords:

runaway electron, radial transport, external helical magnetic field, stochastic magnetic field, JFT-2M tokamak,

1. Introduction

The radial transport of electrons in the stochastic magnetic field has been studied in tokamak plasmas in relation to anomalous transport due to internally excited magnetic fluctuations. The models of the electron behavior in the stochastic magnetic field proposed by Stix[1], Rechester[2] and Krommes[3] assume the motion of electrons along the perturbed magnetic field line. Since the collisional effect on the electron transport is reduced with an increase in electron energy, it is expected that the electron transport must be enhanced due to an increase in the electron velocity along the magnetic field line. On the other hand, some experimental results show a disagreement with the theoretical prediction[4-8]. This disagreement can be explained by the electron centrifugal curvature drift effect[9-11]. However, the effect of the magnetic fluctuation structure on a transport is still not clearly understood yet.

Recently, an experimental studies on the transport of runaway electrons as well as thermal energy in the stochastic magnetic field have been carried out by applying the resonant helical magnetic field with the external local helical coils[12-15]. In the JFT-2M tokamak, the external helical magnetic field has been applied to control the edge plasma transport[16-19] by putting the stochastic magnetic field in the edge plasma region.

This paper deals with the transport enhancement of runaway electrons and also electron thermal energy by applying the external helical field. Especially, the experiments give the diffusion coefficient of runaway electrons and the electron thermal diffusivity in the stochastic magnetic field.

In Section 2, the experimental conditions and techniques are summarized. The experimental results and analyses are presented in Section 3. The electron behavior in the stochastic magnetic field is discussed in Section 4. The final section shows the summary of the experimental results and conclusions taken from the analyses.

2. Experimental Background

The experiments are performed in the JFT-2M tokamak, ohmically heated plasmas with major radius $R_0 = 1.31$m and minor radii $a \times b = 0.33 \times 0.43$m, defined by graphite limiters. Almost all of the vacuum vessel walls are covered with the graphite tiles. Discharge conditions are the central toroidal magnetic field $B_{t0} \sim 1.3$T, the plasma current $I_p \sim 230$kA, the line-averaged electron density $\bar{n}_e \sim 2 \times 10^{19}$m^{-3}, the safety factor at the edge $q_s \sim 4$, and the outermost magnetic surface is determined by the limiter. The location of the helical field coils on the torus can be seen in Fig. 1. Three sets of coils are installed outside of the vessel. The main mode numbers of resonant magnetic island are determined by the current direction flowing in each coil. The poloidal mode structure can be selected to be low m (m = 3-8) or high m mode (m = 10-16), and the toroidal mode can also be chosen in the even or odd mode. The poloidal mode spectrum is relatively broad due to the locality of the helical field coil and has its peak at m = 5 near the plasma surface for the low m case as shown in Fig. 2. The experiment presented here

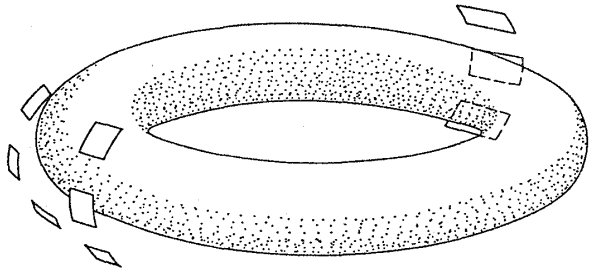

Fig. 1 Location of the helical field coils on the JFT-2M tokamak. Three sets of coils are installed outside the vacuum vessel. The poloidal mode structure can be selected to be low m (m = 3-8) or high m (m = 10-16) mode, and toroidal mode can also be chosen in the even or odd mode.

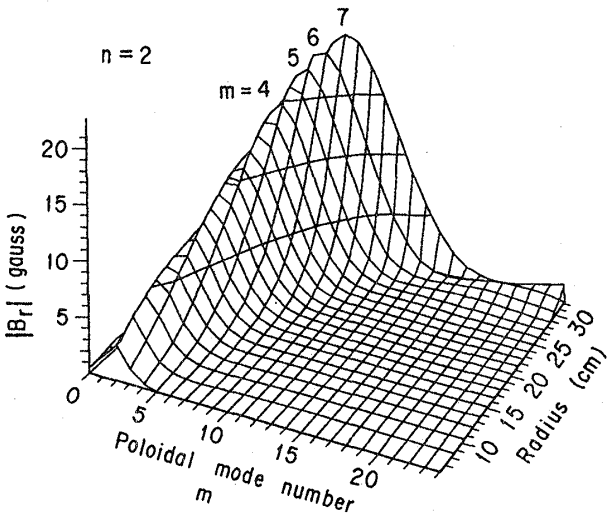

Fig. 2 Profile of the Fourier poloidal mode spectrum for the low m/even n mode.

is performed under the condition of a low m/even n mode.

The runaway electrons with the energy of MeV from plasmas strike the wall or limiter and produce thick target bremsstrahlung radiation. The hard x-ray photons produced have enough energy to pass through the vacuum chamber. We measure these hard x-ray emission proportional to the out-flux of the runaway electrons using the x-ray pulse height analysis system[20]. This is installed at the bottom of vacuum vessel. The detector is made of high purity germanium having a crystal size of 10 mm in diameter and 7mm in depth. The photoelectric effect is strong in the energy regions through 3

to 200 keV. It decreases exponentially outside of the energy window. Although the location of the striking point of runaway electrons is not identified precisely, it seems from another radiation dosimetry measurement to be around the limiter.

Concerning to the thermal energy transport, the electron temperature profile is obtained by electron cyclotron emission (ECE) measurement. The electron density profile is measured using 2 mm microwave interferometer, 3 channel HCN laser interferometer and Langmuir probe.

3. Experimental Results and Analyses

Figure 3(a) shows a typical time evolution of hard x-ray emission in a tokamak discharge accompanied with runaway electrons. The x-ray signals are averaged over several shots. The time resolution is 10 ms. The solid line with open circles corresponds to x-ray emission with the external helical field applied from 600 to 800 ms with a radial field strength of $|B_r|/B_t \sim 2 \times 10^{-3}$ at $r/a \geq 0.8$ (the helical field coil current of $I_h =$ 3.0kA), and the broken line is that without the external helical field. The gradual decrease in the x-ray emission after 500 ms in the discharge without the external helical field indicates that a new runaway source is not likely to grow up. When the external helical field is applied, an initial spike of the emission is observed within 50 ms after the external helical field is turned on (phase I). Just after this, the emission drops sharply from ~6 to ~ 1 kcps with an e-folding time of 18 ms (phase II) and then decay slowly until 800 ms (phase III). A further sudden drop of the emission occurs again just after the helical field is turned off (phase IV).

Such an evolution of x-ray emission can be considered as a result of transport modification of runaway electrons by the stochastic magnetic field. The transport modification for each phase seems as below. The initial spike of phase I shows that the runaway electrons in the edge region are diffused out from the edge stochastic magnetic layer. At this phase, a steep gradient of the runaway profile at the radius around the stochastic boundary r_s is formed. Next, the sharp decrease in phase II shows a lack of the out-flux of the runaway electrons in the stochastic layer. A moderate decrease in phase III shows that the runaway electrons inside r_s are diffusing slowly out to the edge. The process is regulated by the diffusion in the core regions. After the helical field is turned off (phase IV), the stochastic field disappears and the runaway electrons are confined also in the edge region. It causes a sudden drop of x-ray emission.

In phase II and III, the temporal variations of hard x-ray emission are described by exponential decays with two different time constants. For these decreasing phases, we evaluate the diffusion coefficients of runaway electrons using a simple diffusion model. The diffusion equation for runaway electrons in the cylindrical coordinate is given by

$$\frac{\partial N(r,t)}{\partial t} = -\frac{1}{r}\frac{\partial}{\partial r}\left(-rD\frac{\partial N(r,t)}{\partial r}\right) + S_0(r,t) - \frac{N(r,t)}{\tau_s} \qquad (1)$$

with the boundary condition: $N(r=a)=0$, where $N(r,t)$ is the runaway electron density, S_0 is the source term and τ_s is the slowing down time of runaway electrons. Two different diffusion coefficients, D_s and D_b, are assumed in the space as shown in Fig. 3(b). D_s is the diffusion coefficient in the stochastic magnetic field outside of the stochastic boundary r_s and D_b is the coefficient inside r_s. Here, the stochastic boundary is fixed to $r_s/a = 0.8$ determined by the overlapping condition of the neighboring islands[2]. The density profile at $t=0$ is assumed to be $N(r,0) = N_0(1-(r/a)^2)^\alpha$, where α is the power factor of parabolic distribution. The hard x-ray emission is assumed to be proportional to the out-flux of the runaway electrons which is obtained by the volume integral of the first term on right-hand side of Eq. (1). By fitting the measured temporal behavior of the hard x-ray emission with the above numerical analysis, the values of D_s, D_b and α can be determined. The slope of sharp decrease in phase II and that of the moderate decrease in phase III depends dominantly on the values of D_s and D_b, respectively. The decrement of the x-ray emission intensity in these phases is adjusted by changing the α value. The parameters of S_0 and τ_s can not be determined from the present experiment. They are assumed to be $S_0 = 0$ and $\tau_s = 0.7$s. The reason for the assumption

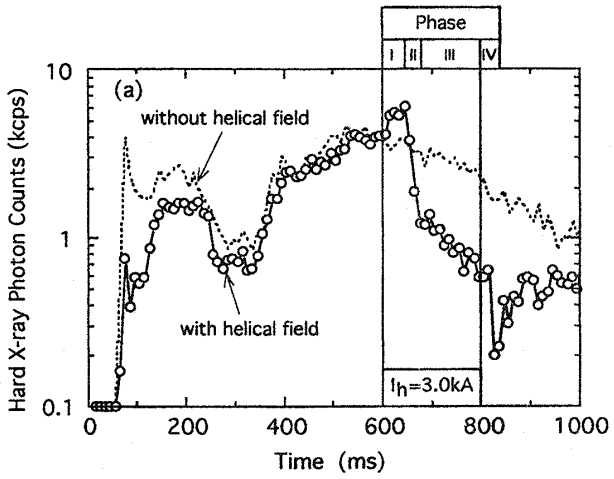

Fig. 3(a) Time evolution of the hard x-ray emission coming from the runaway electrons. The emission intensities are averaged over several shots with a time resolution of 10 ms. The solid line with open circles corresponds to the x-ray emission with an external helical field, and the broken line is that without an external helical field.

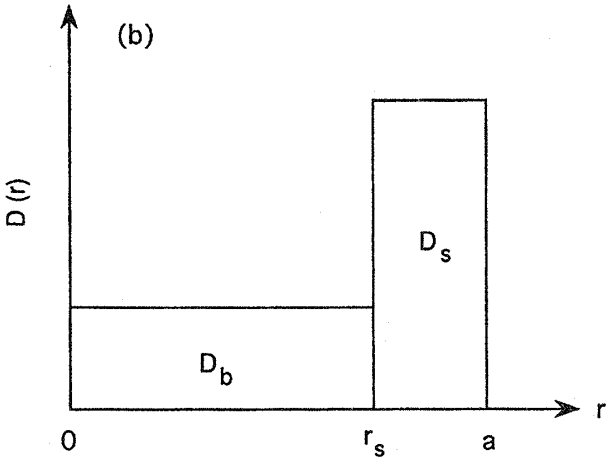

(b) Two area diffusion model for runaway electrons. D_s is the diffusion coefficient in the stochastic magnetic field outside of the stochastic boundary r_s and D_b is the coefficient inside of r_s.

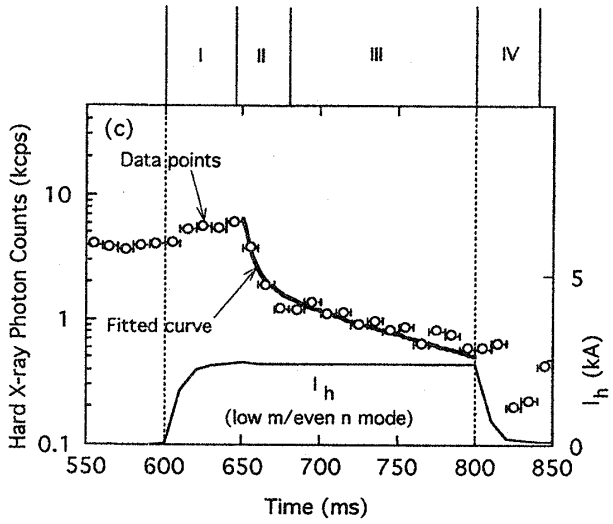

(c) Details of the hard x-ray emission from 550 to 850 ms (open circles) with the helical field. The best fit curve shows the results from the numerical analysis (solid line). The wave form of the helical field coil current is also shown.

of $S_0 = 0$ comes from no grow up of a new runaway source without the external helical field as mentioned initially in this section. In addition it seems that the strong source also does not appear even if the external field is applied because the loop voltage is almost constant before and after the external field is applied, and the hard x-ray emission after the helical is turned off does not return to the level at 500 ms as shown in Fig. 3(a). The value of $\tau_s = 0.7$s corresponds to the slowing down time of about 5 MeV energy electrons by the electron-electron collisions. Figure 3(c) shows a comparison between the observed hard x-ray emission (open circles) and the best fit curve obtained from the numerical analysis (solid line). The wave form of the helical field coil current is also provided here. The curve fitting is done from 650 to 800 ms. The best fitting gives the values of $Ds = 1.0 \pm 0.2\mathrm{m}^2/\mathrm{s}$, $D_b = 0.1 \pm 0.05\mathrm{m}^2/\mathrm{s}$ and $\alpha = 1.5 \pm 0.5$ on the fixed parameters of $r_s/a = 0.8$, $S_0 = 0$ and $\tau_s = 0.7$s.

D_s is not affected significantly by any of the values of r_s, S_0 and τ_s. For example, changing the value of r_s/a through 0.7 to 0.9, the best fitting is given by $D_s = 1.2\text{-}0.8\mathrm{m}^2/\mathrm{s}$, $D_b = 0.07\text{-}0.11\mathrm{m}^2/\mathrm{s}$ and $\alpha = 2.5\text{-}1.0$. Since parameters α and D_b depend on S_0 and τ_s, respectively, some ambiguity for determining α and D_b still remains. In the present analysis, D_s can be determined clearly at least. The diffusion coefficient of the runaway electrons in the discharge without the helical field is also evaluate by using the same model with a constant diffusion coefficient in space. The value thus evaluated is $\sim 0.07\mathrm{m}^2/\mathrm{s}$ which is almost same as the value of D_b.

Next, concerning to the electron thermal

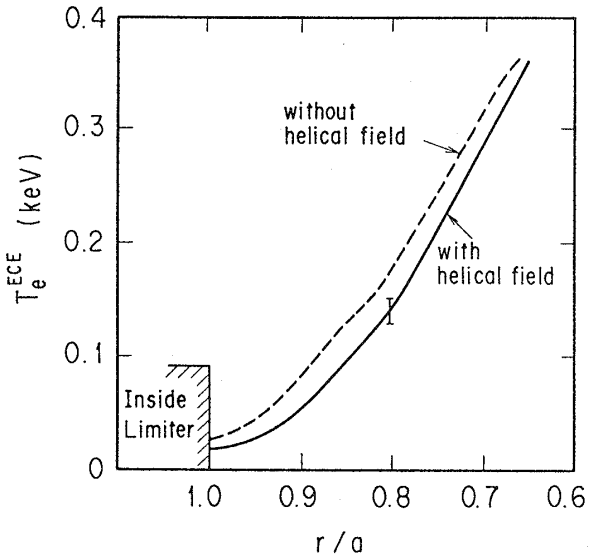

Fig. 4 Electron temperature profiles from ECE in the discharge with an external helical field at low m/even n and $I_h = 3$kA. The solid line and broken line show the cases with and without the helical field.

diffusivity, the electron temperature profile was measured by ECE in discharge with the external helical field at low m/even n and $I_h = 3$kA as shown in Fig. 4. The solid and broken lines give the profiles with and without an external helical field, respectively. A decrease in the electron temperature is observed by applying the helical field. Especially, the temperature gradient becomes small at $r/a \geq 0.9$. The electron density profile is almost constant. This reduction of radial T_e gradient shows the enhancement of the edge electron thermal diffusivity due to the external helical field.

By using the profiles of electron temperature and density at the edge, the local electron thermal diffusivity $\chi_{eff} \sim q_{the}/(-2n\partial T_e/\partial r)$ is estimated. The thermal heat flux q_{the} is given as $q_{the} = (1/r) \cdot \int_0^r r^* P_{in} dr^*$, where input power P_{in} is determined by subtracting the radiation loss from the ohmic heating power. The electron thermal diffusion coefficient is evaluated at $r/a = 0.95$ where the change in temperature gradient is large. The value of $\chi_{eff} \sim 20 m^2/s$ thus evaluated is about twice as large as that without the external helical field.

4. Discussions

4.1 Diffusion coefficient from collisionless/collisional model

The magnetic field diffusion coefficient is defined from the field line excursion according to Rechester and Rosenbluth as $D_m = \langle(\Delta r)^2\rangle / 2L$[2], where $\langle(\Delta r)^2\rangle$ is the mean squared radial displacement and L is the path length of the field line. The magnetic field line tracing code for JFT-2M was developed to obtain the magnetic field structure: island width, mode structure and field line diffusion coefficient. The perturbed magnetic field generated by the local helical field is combined with the unperturbed equilibruum magnetic field. This *sophisticated code* gives a value with a field line diffusion coefficient of about $D_m = 3 \times 10^{-5}$m in the edge stochastic magnetic field at the condition of low m/even n mode with $n \leq 6$ and $I_h = 3.0$kA.

The electron heat diffusivity in the stochastic magnetic field has been estimated from the field line diffusion coefficient by Stix[1], Rechester[2] and Kadomtsev[21]. Each model has an applicable regime depending on electron temperature, electron density, electron velocity, q-value, q-profile, and machine size (major and minor radii). The applicable regime is summarized in Ref. 12. Taking into account of the JFT-2M experimental condition, the collisionless Rechester model[2] is the most appropriate to deduce the diffusion coefficient of runaway electrons (D_s^{cl}), whereas the collisional Rechester model[2] can be used for the electron thermal diffusivity (χ_e^c). The runaway electron diffusion coefficient for the collisionless Rechester model is represented as $D_s^{cl} = D_m v_{//}$, where $v_{//}$ is the parallel component of electron velocity. For runaway electrons with MeV energy, D_s^{cl} is estimated to be $\sim 10^4 m^2/s$ by using the value of $D_m = 3 \times 10^{-5}$m. The value of $D_s^{cl} \sim 10^4 m^2/s$ is four orders of magnitude larger than the value of $D_s = 1 m^2/s$ obtained experimentally. On the other hand, the electron thermal diffusivity for the collisional Rechester model is represented $\chi_e^c = D_m D_{//}/L_k$, where $D_{//}$ is the parallel electron diffusion coefficient ($= v_{the}^2/\nu$ with the thermal electron velocity v_{the} and the Coulomb collision frequency ν) and $L_k = L_s^{2/3} L_\perp^{1/3}$, with the shear length L_s and $L_\perp = (D_m \sum_m (m/a)^2)^{-1}$. The value deduced at $r/a = 0.95$ ($T_e \sim 30$eV and $n_e \sim 4 \times$

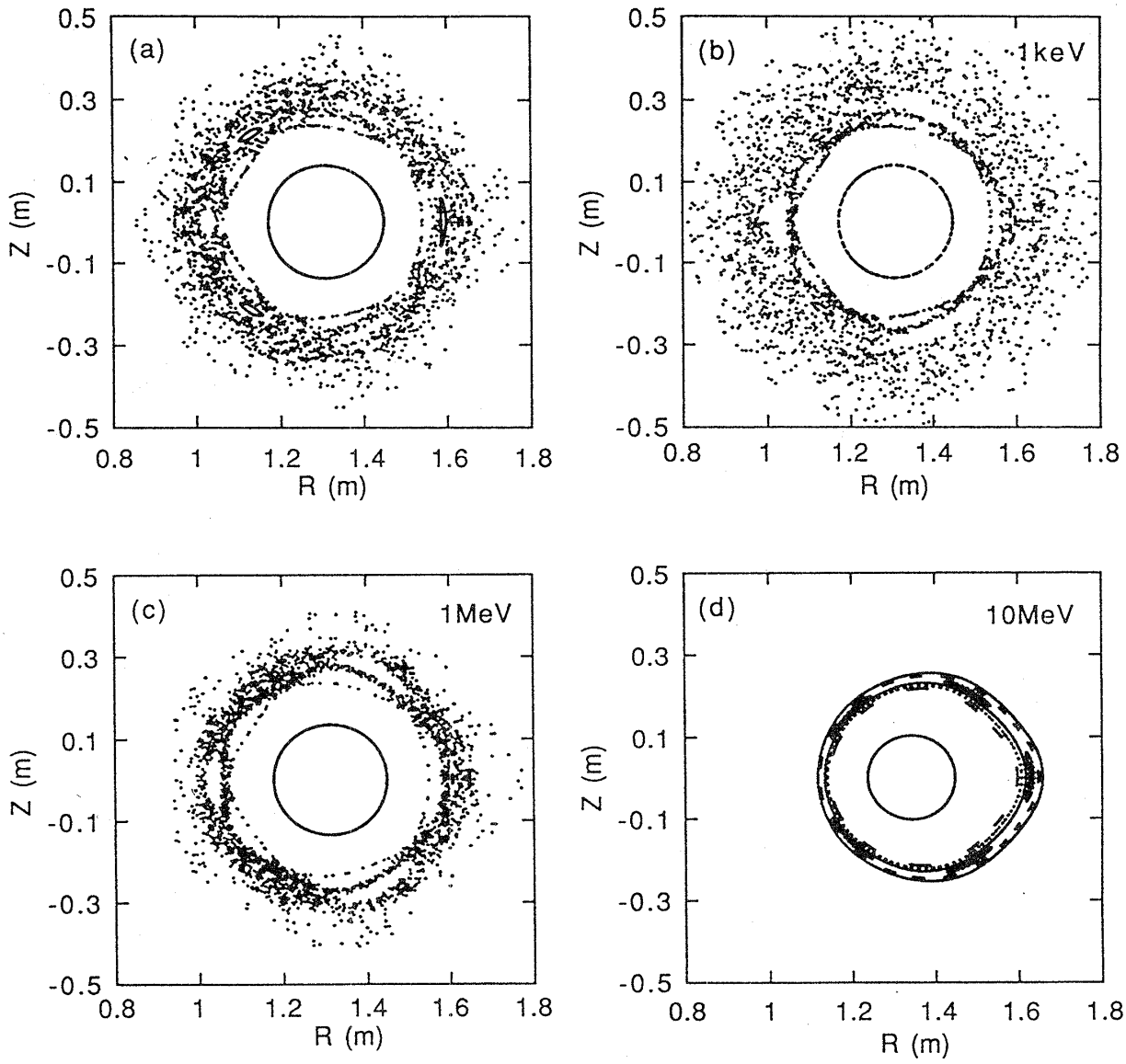

Fig. 5(a) Puncture plot of the magnetic field line on the poloidal cross section. The analytic perturbed radial field B_r^a is applied and the parameters of $R_0 = 1.31$m, $a = 0.35$m, $B_{t0} = 1.3$T, $q_s = 4$ and $q(r) = 1 + 3(r/a)^2$ are used. The starting points for field line tracing are taken to $R = 1.45, 1.60, 1.61, 1.62, 1.63, 1.64, 1.65$ and 1.66m, $\varphi = 0°$ and $Z = 0$m, respectively. The total number of toroidal turns is 500.
(b)-(d) Puncture plots of the drift orbits of electrons with energies of 1 keV, 1 MeV and 10 MeV under the same condition as (a).

$10^{18}\mathrm{m}^{-3}$) is $\chi_e^c \sim 30\mathrm{m}^2/\mathrm{s}$. It is not very much different from the experimental value of $\chi_{eff} \sim 20\mathrm{m}^2/\mathrm{s}$.

4.2 Electron orbit calculation in the stochastic magnetic field

We discuss the relation of $D_s \ll D_s^{cl}$ in Section 4. 1 in terms of the orbit motion for high energy electrons in the edge stochastic magnetic field [10,22]. In order to evaluate the runaway electron transport in the stochastic magnetic field, the guiding center drift orbit of the relativistic electron is calculated by the *simplified code*, in which the analytic form for the perturbed radial field B_r^a given by the following formula is used,

$$B_r^a(r) = \sum_m b(m, r_k) \left(\frac{r}{r_k}\right)^{m-1} \sin(m\theta - n\varphi + \Delta_m) \qquad (2)$$

where $b(m, r_k) = w^2 \cdot m \cdot q' \cdot B_\theta / 16 \cdot r_k \cdot q$ [23] with island width w, poloidal magnetic field B_θ and the

resonance position r_k on q-surface. The island mode of $m=4$-8 and $n=2$ and $w/a=0.1$ are used to model the present stochastic magnetic field. The stochastic magnetic layer is constructed between $r/a\sim0.8$ and $r/a\sim1$. Figure 5 (a) shows the puncture plot of the magnetic field line on the poloidal cross section. Peripheral scattered points show that magnetic surfaces are destroyed by the overlapping of the neighboring islands. Figures 5 (b) to 5 (d) also show the puncture plots of drift orbits of electrons with energies of 1 keV, 1 MeV and 10 MeV, respectively. Here, the electron has mono energy with a zero pitch angle and the electric field is ignored. Eight electrons with each energy start at the outer midplane ($R=1.45$, 1.60, 1.61, 1.62, 1.63, 1.64, 1.65 and 1.66m). The wide region consisting of peripheral scattered points related to the stochastic magnetic field can be seen in the structure of puncture plot for 1 keV electrons. For 1 MeV electrons, the region of scattered points becomes much narrower than that for 1 keV electrons. For 10 MeV electrons, such a scattering is greatly suppressed.

In the edge regions, the motion of thermal electrons is very sensitive to the local fine structure of the magnetic field lines, whereas the drift orbit of the high energy electrons accompanied with higher parallel velocity is greatly displaced from the intrinsic magnetic surface due to the large toroidal drift. It gives a substantial reduction in their path length on which the high energy electrons experience in their drift motion. It means that a part of path is in the unperturbed central regions. In addition, the larger mismatching between the drift orbit and the magnetic surface gives a phase averaging effect by passing through the area with a different sign of B_r. Therefore, even if the stochastic magnetic field structure is constructed in the edge plasma regions, the high energy electrons do not follow the local fine magnetic field lines and they pass through such regions without any significant perturbation.

The mean squared radial displacement $\langle(\Delta r)^2\rangle$ of magnetic field line as well as electron orbit in the stochastic magnetic field is obtained numerically to represent quantitatively the stochasticity of the motion of the high energy electrons. Figures 6 (a) and 6 (b) show $\langle(\Delta r)^2\rangle$ as a function of number of

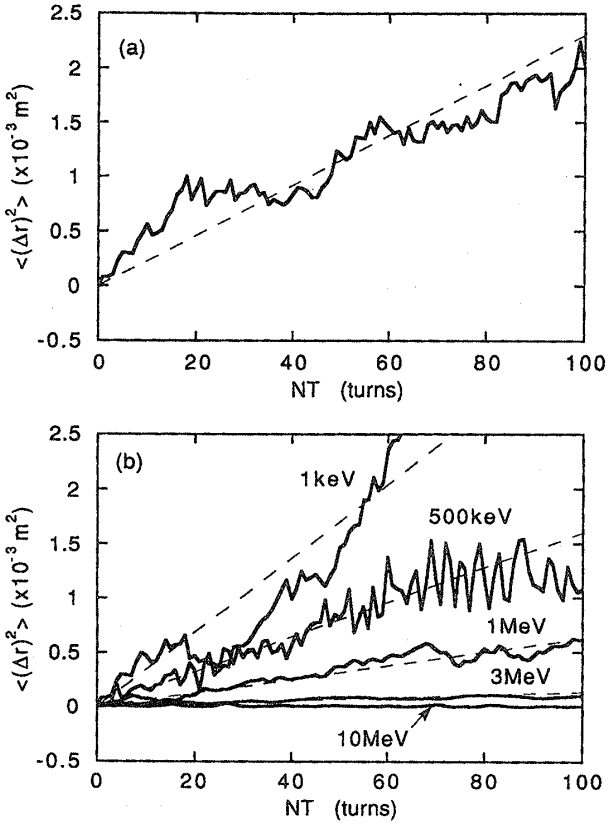

Fig. 6 Mean squared radial displacement $\langle(\Delta r)^2\rangle$ of magnetic field line (a) and drift orbits of electrons with several energies (b) in the stochastic magnetic field as a function of number of toroidal turn NT.

toroidal turn NT for the magnetic field line and the drift orbits of electrons with several energies, respectively. The number of toroidal turn for magnetic field line is a measure of the length along the field line. Magnetic field line tracing gives linear increase for $\langle(\Delta r)^2\rangle$ with NT. This indicates that the stochasticity of the magnetic field line at the edge is described as a diffusion process. For the electron orbit, $\langle(\Delta r)^2\rangle/\mathrm{NT}$ decreases as the electron energy increases. Then, it becomes very small with the energy over ~1 MeV as seen in Fig. 7. Thus, the effect of the edge stochastic magnetic field on the electron diffusivity with MeV energy electrons becomes much smaller than that of the thermal electrons. This dependence provides a comprehensive reason for the large difference between D_s and D_s^{cl}.

Rechester model of transport due to magnetic stochasticity assumes that an electron runs along a perturbed magnetic field line. This assumption of

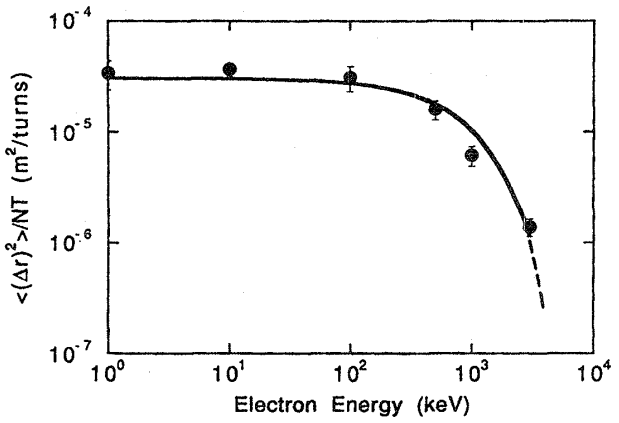

Fig. 7 Electron energy dependence of $\langle(\Delta r)^2\rangle/NT$.

negligible drifts leads to the expectation that the high energy electrons are diffused much more effectively than the thermal electrons due to a reduction of their collisional effect. In contrast with this expectation, we show here that the diffusion of the high energy electrons by taking into account of their large toroidal drift motion becomes much smaller than that of the thermal electrons in the edge stochastic magnetic field.

4. 3 Runaway electron diffisivity in the unperturbed regions

In Section 3, we have estimated by the analysis of the experiment that the diffusion coefficient of the runaway electrons in the edge stochastic magnetic field is nearly an order of magnitude greater than in the unperturbed region. Although the diffusion of runaway electrons in such a stochastic field is greatly reduced from the value estimated Rechester model, there is a still remaining weak stochasticity of electron motion, which is able to give the enhancement of diffusion of runaway electrons in the stochastic field compared with that of those in unperturbed region.

If we assume that the radial diffusion of the runaway electrons in the unperturbed regions is dominated by the internally excited magnetic fluctuation, the radial field strength is estimated to be $|B_r|/B_t \sim 6 \times 10^{-4}$ which seems to be too large for a normal ohmic discharge. In the present experiment, it is not known what determines the runaway electron transport in the unperturbed regions. A further investigation will be necessary to understand the electron transport in the perturbed magnetic field.

5. Summary and Conclusions

In the experiments with the externally applied helical magnetic field in the JFT-2M tokamak, it is shown that the transport of both runaway electrons and electron thermal energy is enhanced significantly by applying the external helical magnetic field.

The diffusion coefficient of runaway electrons is analyzed from the temporal behavior of the hand x-ray emission using a simple diffusion model. With the radial field strength $|B_r|/B_t \sim 2 \times 10^{-3}$, the model fitting gives the runaway electron diffusion coefficient of about $D_s = 1\mathrm{m}^2/\mathrm{s}$ in the edge stochastic magnetic field, the value of which is much larger than that in the unperturbed regions.

The diffusion coefficient of runaway electrons, estimated from the collisionless Rechester model, is about four orders of magnitude larger than the value of D_s obtained experimentally. A possible reason for such a large difference is that the high energy electrons accompanied with higher parallel velocity are not affected significantly by the edge stochastic magnetic field due to their large toroidal drift motion. A numerical analysis on the motion of high energy electrons in the stochastic magnetic field shows that the stochastic effects of the magnetic field lines are greatly suppressed for high energy electrons,and the stochasticity of their orbit is smoothed out as the energy increases.

On the other hand, the thermal diffusivity is evaluated from the edge electron temperature profile. The analysis gives $\chi_{eff} \sim 20\mathrm{m}^2/\mathrm{s}$ at $r/a = 0.95$ on the stochastic magnetic field in the presence of the helical field. This value is about twice larger than that without the external helical field. The thermal energy transport is sensitively affected by the stochastic magnetic field since the thermal electrons follow the magnetic field lines even for the local fine structure owing to the small shift of drift surface from their own magnetic surface.

Acknowledgments

This work is supported by a joint study between Japan Atomic Energy Research Institute and Nagoya University.

The authors would like to thank the JFT-2M operating group for their excellent support for this work. They are also grateful for the continued

support from Drs. H. Maeda, H. Kishimoto and S. Tamura of the Japan Atomic Energy Research Institute.

References

[1] T. H. Stix, Nucl. Fusion **18**, 353 (1978).
[2] A. B. Rechester and M. N. Rosenbluth, Phys. Rev. Lett. **40**, 38 (1978).
[3] J. A. Krommes, C. Oberman and R. G. Kleva, J. Plasma Phys. **30**, 11 (1983).
[4] S. von Goeler, W. Stodiek, N. Sauthoff and H. Selberg, Presented at the *Third International Symposium on Toroidal Plasma Confinement*, Max-Planck Institute for Physik, Garhing (1973), paper B-25.
[5] J. D. Strachan, E. B. Meservey, W. Stodiek, R. A. Naumann and F. Girshick, Nucl. Fusion **17**, 140 (1977).
[6] V. V. Alikaev, G. A. Bobrovskii, V. I. Poznyak, K. A. Razumova, V. V. Sannikov, Yu. A. Sokolov and A. A. Shmarin, Sov. J. Plasma Phys. **2**, 212 (1976).
[7] S. J. Zweben, D. W. Swain and H. H. Fleischmann, Nucl. Fusion **18**, 1679 (1978).
[8] O. J. Kwon, P. H. Diamond, F. Wagner, G. Fussmann, ASDEX and NI team, Nucl. Fusion **28**, 1931 (1988).
[9] H. E. Mynick and J. D. Strachan, Phys. Fluids **24**, 695 (1981).
[10] S. J. Zweben, B. V. Waddel, D. W. Swain and H. H. Fleischmann, Nucl. Fusion **20**, 477 (1980).
[11] H. Knoepfel and D. A. Spong, Nucl. Fusion **19** 785 (1979).
[12] S. C. McCool, A. J. Wootton, A. Y. Aydemir, R. D. Bengtson, J. A. Boedo, R. V. Bravenec, D. L. Brower, J. S. DeGrassie, T. E. Evans, S. P. Fan, J. C. Forster, M. S. Foster, K. W. Gentle, Y. X. He, R. L. Hickock, G. L. Jackson, S. K. Kim, M. Kotshenreuther, N. C. Luhmann, Jr., W. H. Miner, Jr., N. Ohyabu, D. M. Patterson, W. A. Peebles, P. E. Phillips, T. L. Phodes, B. Richards, C. P. Ritz, D. W. Ros, W. L. Rowan, P. M. Schoch, B. A. Smith, J. C. Wiley, X. H. Yu and S. B. Zheng, Nucl. Fusion **29**, 547 (1989).
[13] P. Deschamps, A. Grosman, M. Lipa and A. Samain, J. Nucl. Mater. **128**, 38 (1984).
[14] S. Takamura, N. Ohnishi, H. Yamada and T. Okuda, Phys. Fluids **30**, 144 (1987).
[15] P. J. Catto, J. R. Myra, P. W. Wang, A. J. Wootton and R. D. Bengtson, Phys. Fluids **B3**, 2038 (1991).
[16] T. Shoji, T. Fujita, M. Mori, A. M. Howald, A. W. Leonard, N. Ohyabu, H. Tamai, H. Aikawa, K. Hoshino, K. Ida, S. Kasai, T. Kawakami, H. Kawashima, H. Maeda, T. Matsuda, Y. Miura, K. Odajima, H. Ogawa, S. Sengoku, N. Suzuki, T. Yamamoto, T. Yamauchi, T. Hamano, K. Hasegawa, A. Honda, I. Ishibori, M. Kazawa, Y. Kashiwa, K. Kikuchi, F. Okano, T. Shibata, T. Shiina, K. Suzuki, T. Tokutake and S. Uno, in *Cotrolled Fusion and Plasma Physics* (Proc. 17th. Europ. Conf. Amsterdam, 1990) Part III, European Physical Society, 1452 (1990).
[17] H. Tamai, T. Shoji, M. Mori, Y. Miura, T. Fujita and G. Fuchs, *Japan Atomic Energy Research Institute Report* JAERI-M 91-110 (1991).
[18] Y. Miura, H. Aikawa, K. Hoshino, S. Kasai, T. Kawakami, H. Kawashima, H. Maeda, T. Matsuda, M. Mori, K. Odajima, H. Ogawa, S. Sengoku, M. Shimada, T. Shoji, N. Suzuki, H. Tamai, S. Tsuji, T. Yamamoto, T. Yamauchi, T. Fujita, A. M. Howald, A. W. Hyatt, K. Ida, A. W. Leonard, N. Ohyabu, S. Gunji, T. Hamano, K. Hasegawa, A. Honda, I. Ishibori, Y. Kashiwa, M. Kazawa, K. Kikuchi, F. Okano, E. Sato, N. Seki, T. Shibata, T. Shiina, K. Suzuki, S. Suzuki, T. Tokutake and S. Uno, in *Plasma Physics and Controlled Nuclear Fusion Research* (Proc. 13th int. Conf., Washington, 1990), Vol. 1, IAEA, Vienna, 325 (1991).
[19] M. Mori, H. Aikawa, Y. Asahi, T. Fujita, K. Hoshino, S. Kasai, T. Kawakami, H. Kawashima, H. Maeda, K. Maeno, T. Matsuda, Y. Miura, K. Odajima, H. Ogawa, T. Seike, T. Shiina, T. Shoji, H. Tamai, K. Uehara, T. Yamauchi, K. Hasegawa, A. Honda, Y. Kashiwa, K. Kikuchi, M. Komata, Y. Matsuzaki, F. Okano, M. Saito, E. Sato, N. Seki, T. Shibata, N. Suzuki, S. Suzuki, T. Tani, T. Tokutake, Y. Tomiyama, T. Yamazato, Y. Sakuragi, Z. Yoshida, N. Inoue, A. W. Leonard, T. Jensen, B. M. Annaratone and K. Ida, in *Plasma Physics and Controlled Nuclear Fusion Research* (Proc. 14th Int. Conf., Wurzburg, 1992), Vol. 2, IAEA, Vienna, 567 (1993).
[20] H. Kawashima, T. Matoba and JFT-2M Group, Rev. Sci.Instrum. **59**, 1816 (1988).
[21] B. B. Kadomtsev and O. P. Pogutse, in *Plasma Physics and Controlled Fusion and Plasma Physics (Proc. 14th Eur. Int. Conf. Innsbruck, 1979)*, Vol. 1, IAEA, Vienna, 649 (1979).
[22] S. Sakurai and S. Takamura, Kakuyugo Kenkyu **68**, 34 (1992).
[23] J. Wesson, *Tokamaks* (Clarendon Press, Oxford, 1987) p. 169.